JOURNAL OF VIROLOGY, Dec. 2002, p. 12513–12525 Vol. 76, No. 24
0022-538X/02/$04.00+0 DOI: 10.1128/JVI.76.24.12513–12525.2002

Mechanism of De Novo Initiation by the Hepatitis C Virus RNA-Dependent RNA Polymerase: Role of Divalent Metals

C. T. Ranjith-Kumar,[1] Young-Chan Kim,[1] Les Gutshall,[2] Carol Silverman,[2] Sanjay Khandekar,[2] Robert T. Sarisky,[2] and C. Cheng Kao[1]*

Department of Biology, Indiana University, Bloomington, Indiana 47405,[1] and Department of Virology, The Metabolic and Antiviral Diseases Center of Excellence for Drug Discovery, GlaxoSmithKline Pharmaceuticals, Collegeville, Pennsylvania 19426[2]

Received 7 May 2002/Accepted 10 September 2002

We functionally analyzed the role of metal ions in RNA-dependent RNA synthesis by three recombinant RNA-dependent RNA polymerases (RdRps) from GB virus-B (GBV), bovine viral diarrhea virus (BVDV), and hepatitis C virus (HCV), with emphasis on the HCV RdRp. Using templates capable of both de novo initiation and primer extension and RdRps purified in the absence of metal, we found that only reactions with exogenously provided Mg^{2+} and Mn^{2+} gave rise to significant amounts of synthesis. Mg^{2+} and Mn^{2+} affected the mode of RNA synthesis by the three RdRps. Both metals supported primer-dependent and de novo-initiated RNA by the GBV RdRp, while Mn^{2+} significantly increased the amount of de novo-initiated products by the HCV and BVDV RdRps. For the HCV RdRp, Mn^{2+} reduced the K_m for the initiation nucleotide, a GTP, from 103 to 3 μM. However, it increased de novo initiation even at GTP concentrations that are comparable to physiological levels. We hypothesize that a change in RdRp structure occurs upon GTP binding to prevent primer extension. Analysis of deleted proteins revealed that the C terminus of the HCV RdRp plays a role in Mn^{2+}-induced de novo initiation and can contribute to the suppression of primer extension. Spectroscopy examining the intrinsic fluorescence of tyrosine and tryptophan residues in the HCV RdRp produced results consistent with the protein undergoing a conformational change in the presence of metal. These results document the fact that metal can affect de novo initiation or primer extension by flaviviral RdRps.

Polymerases are metal-activated enzymes that use divalent metals for nucleotide polymerization. The paradigm for catalysis by DNA-dependent RNA polymerases is that two Mg^{2+} ions coordinate the nucleotides and catalyze the formation of the phosphodiester bonds (11). These metals are specifically recognized by amino acids in the catalytic pocket of the polymerase.

RNA viruses can initiate RNA synthesis by a number of mechanisms. Many use a de novo initiation mechanism in which the first phosphodiester bond is formed between the initiation nucleotide, usually a purine triphosphate, and a second nucleoside triphosphate (NTP). Others, such as poliovirus, use a primer-dependent mechanism (25). Yet others, such as the influenza virus, can use a combination of the two strategies, depending on the RNA to be synthesized (8). *Flaviviridae* RNA-dependent RNA polymerases (RdRps) can initiate RNA synthesis by a de novo mechanism (12, 13, 14, 21, 23, 33, 40). De novo initiation is likely the mechanism used during flavivirus replication in vivo (3, 13). The hepatitis C virus (HCV) nonstructural protein 5B (NS5B), the RdRp, has a β-loop near the catalytic pocket (4, 18) that has been proposed to discriminate against primer extension and to provide at least part of the structural basis for de novo initiation (9). Despite the presence of the β-loop, the HCV and other flaviviral RdRps are capable of primer extension. In fact, primer extension is so robust that de novo initiation of RNA synthesis was not observed in some early studies (2, 7, 19, 20, 38). These results beg the question of how primer extension and de novo initiation are differentially achieved by the same recombinant flaviviral RdRps.

In RNA synthesis assays, the addition of 1 to 2 mM Mn^{2+} to a reaction mixture containing Mg^{2+} increased RNA synthesis, while higher concentrations tended to be inhibitory (7, 21). Mn^{2+} has been reported to affect several polymerase activities, such as decreasing the specificity for the template and in nucleotide incorporation, lowering the K_m for template binding, and increasing terminal nucleotide addition (24, 29, 34, 35, 37). These observations and the low physiological concentration of Mn^{2+} led some researchers to rule out a role for Mn^{2+} in the normal mechanism of viral RNA synthesis in the infected cell.

There is some suggestive evidence that Mn^{2+} may play a more active role in RNA-dependent RNA synthesis in at least some RdRps. The crystal structures of the RdRp from phage ϕ6 can, in the absence of NTPs, bind either Mg^{2+} or Mn^{2+} at a site approximately 6 Å from the catalytic aspartate residues, an unexpected feature in comparison to other polymerases (5). In the presence of nucleotide, the crystal structure of the RdRp from a calicivirus can form a closed and presumably active structure in the presence of two Mn^{2+} ions (22). Mn^{2+} also has a higher occupancy rate in the HCV RdRp than Mg^{2+} (3).

Using a template capable of both de novo initiation and primer extension, we found that Mn^{2+} is strongly preferred for de novo initiation by the HCV RdRp and increases de novo

* Corresponding author. Mailing address: Department of Biology, Indiana University, 1001 E. Third St., Bloomington, IN 47405. Phone: (812) 855-7959. Fax: (812) 855-6705. E-mail: ckao@bio.indiana.edu.

initiation by the RdRp from bovine viral diarrhea virus (BVDV). In contrast, the HCV RdRp preferentially performed primer extension in the presence of Mg^{2+}. Analysis of C-terminally truncated HCV RdRps revealed that the C-terminal portion of the RdRp contributes to Mn^{2+}-dependent de novo initiation and the suppression of primer extension. Spectroscopy examining the intrinsic fluorescence of tyrosine and tryptophan residues in the HCV RdRp confirms that the presence of Mg^{2+} or Mn^{2+} resulted in a spectral change in the protein.

MATERIALS AND METHODS

Purification of NS5B from *Escherichia coli*. NS5B proteins were expressed in fermentors from pET derivatives of *E. coli* BL21(DE3)LysS. NS5B proteins from HCV, BVDV, and GB virus-B (GBV) were truncated at their C termini by 21, 23, and 23 amino acids, respectively. In addition, six histidines were added to the C termini of each of the proteins to allow affinity purification. Bacteria were grown at 30°C in standard Luria-Bertani medium supplemented with ampicillin and chloramphenicol at 50 and 34 μg/ml, respectively, until the culture reached an optical density at 600 nm of 1.0. The culture temperature was then lowered to 25°C, and expression was induced for 4 h with 1 mM isopropyl-thiogalactoside. Cells were harvested after centrifugation, and recombinant RdRps from HCV, BVDV, and GBV were purified in buffer lacking divalent metals by passage through a Talon nickel-affinity column (Invitrogen, Inc., San Diego, Calif.) followed by passage through a poly(U)-agarose column (Pharmacia Inc). The proteins were adjusted to between 1 and 2 mg/ml after quantification by the Lowry assay with bovine serum albumin as a concentration control. N termini of the expressed proteins were sequenced to confirm the correct translation of each protein.

RdRp activity assays. RNAs were chemically synthesized by Dharmacon, Inc. (Boulder, Colo.), purified by denaturing gel electrophoresis, checked for quality by toluidine blue staining, and quantified by spectrophotometry. Standard RdRp assays consisted of a 0.125 μM concentration of template (unless stated otherwise) with 0.08 μM NS5B in a 20-μl reaction mixture containing 20 mM sodium glutamate (pH 8.2), 12.5 mM dithiothreitol, 0.5% (vol/vol) Triton X-100, 200 μM ATP and UTP, 200 μM GTP, and 250 nM [α-^{32}P]CTP (Amersham, Inc.). $MgCl_2$ or $MnCl_2$ was added to a final concentration of 2 mM unless otherwise stated. Due to the buffer used to store the RdRp, the final reaction mixture also contains 10 mM NaCl. RNA synthesis reaction mixtures were incubated at 25°C for 60 min and stopped by phenol-chloroform extraction followed by ethanol precipitation in the presence of 5 μg of glycogen and 0.5 M ammonium acetate. Assays monitoring the effects of temperature were mixed on ice and transferred to different water baths maintained at the indicated temperatures. Products were usually separated by electrophoresis on denaturing (7.5 M urea) polyacrylamide gels. Gels were wrapped in plastic and exposed to film at −80°C. Each result shown has been reproduced in at least one (usually two to four) other independent experiment. Quantification of radiolabeled bands was performed using a PhosphorImager (Molecular Dynamics, Piscataway, N.J.).

The kinetic constant K_m was determined by using the assay described above. To prevent reinitiation and thereby determine the initial reaction rates, heparin (to 0.5 mg/ml) and 50 μM nonradiolabeled CTP was added to the reaction mixture after 10 min of incubation. The substrate concentrations ranged from 2 to 100 μM in the presence of Mn^{2+} and 2 to 1,000 μM in the absence of Mn^{2+}. The reaction products were quantified and plotted using Cricket Graph, and the K_m value was determined from the x intercept.

Nondenaturing gel electrophoresis. While LE19 and LE21 are expected to have minimally stable RNA structures, their structures were examined using a native gel electrophoresis assay that can detect the formation of higher-orders structures (32). In some of the reaction mixtures, 2 mM Mn^{2+}, Mg^{2+} or both were added to the RNAs to assess whether there is an influence on the structures of the RNAs. All reactions contained 10 μM RNA and 100 mM KCl. The RNAs were detected by staining with toluidine blue.

Tryptophan and tyrosine fluorescence spectroscopy. Measurements were performed using a Perkin-Elmer GmbH (Wellesley, Mass.) LS50 spectrofluorometer. For tryptophan fluorescence measurements, the excitation wavelength was set at 295 nm and the emission spectra were recorded from 300 to 400 nm with a 5-nm bandwidth of excitation and emission. For tyrosine fluorescence measurements, the excitation wavelength was set at 275 nm and the emission spectra were recorded from 285 to 400 nm with a 5-nm bandwidth of excitation and emission. All measurements were done at 4°C and repeated at least twice and averaged. HCV NS5B Δ21 (1 μM) and Mg^{2+} or Mn^{2+} at the specified final concentrations were diluted with a buffer containing a final concentration of 50 mM HEPES (pH 7.5), 300 mM NaCl, and 1 mM dithiothreitol.

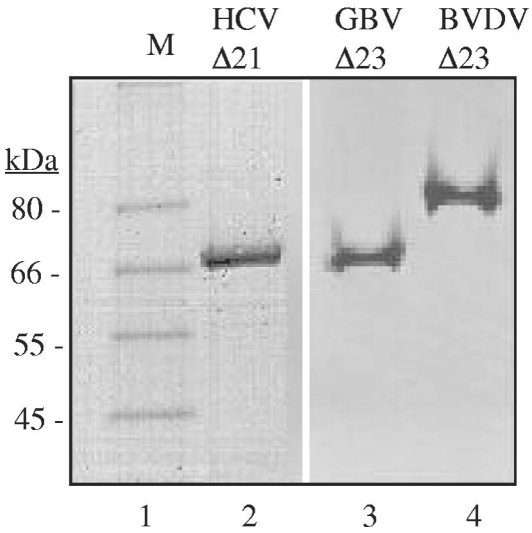

FIG. 1. Recombinant proteins used in the study. The proteins were separated on a sodium dodecyl sulfate–10% polyacrylamide gel and stained with Coomassie brilliant blue. Purified RdRps are identified above the image of the gel. M denotes the molecular weight marker from Invitrogen, Inc.

RESULTS

De novo initiation and primer dependent RNA synthesis. Recombinant RdRps from HCV, GBV, and BVDV were purified to single band in a Coomassie blue-stained gel (Fig. 1). Characterization of de novo-initiated RNA synthesis by the HCV and BVDV RdRps has been reported earlier (14, 16, 40). The GBV RdRp was demonstrated to initiate RNA synthesis by a de novo mechanism and to extend from a primer (C. T. Ranjith-Kumar, J. Lin-Goerke, L. A. Gutshall, et al, unpublished data).

RNA synthesis assays primarily used a 19-nucleotide (nt) RNA, LE19 (Fig. 2A), whose sequence is derived from the 3′ end of the minus-strand BVDV genome. There are many reasons for using LE19. First, since it has only one cytidylate at the initiation position, LE19 allows us to use GTP only for initiation and not for elongation. Second, as will be shown in this work, it directs robust levels of RNA synthesis by all three recombinant RdRps. Third, LE19 can be used to detect four RdRp activities within the same reaction: de novo initiation, primer extension, terminal transferase activity (29), and RNA template switch leading to the formation of recombinant products (15). Terminal transferase activity would add nontemplated nucleotides to LE19, resulting in products longer than 19 nt. De novo initiation from the 3′-terminal cytidylate that terminated at the 5′ end of LE19 would result in a 19-nt newly synthesized RNA. Should the de novo-initiated ternary complex not terminate and use a second template to continue synthesis (as shown in reference 15), the product of this template switch event will be ca. 38 nt long. Finally, should two LE19 molecules anneal through six base-paired nucleotides involving the 3′ ends of the RNAs (Fig. 2A, schematic on the

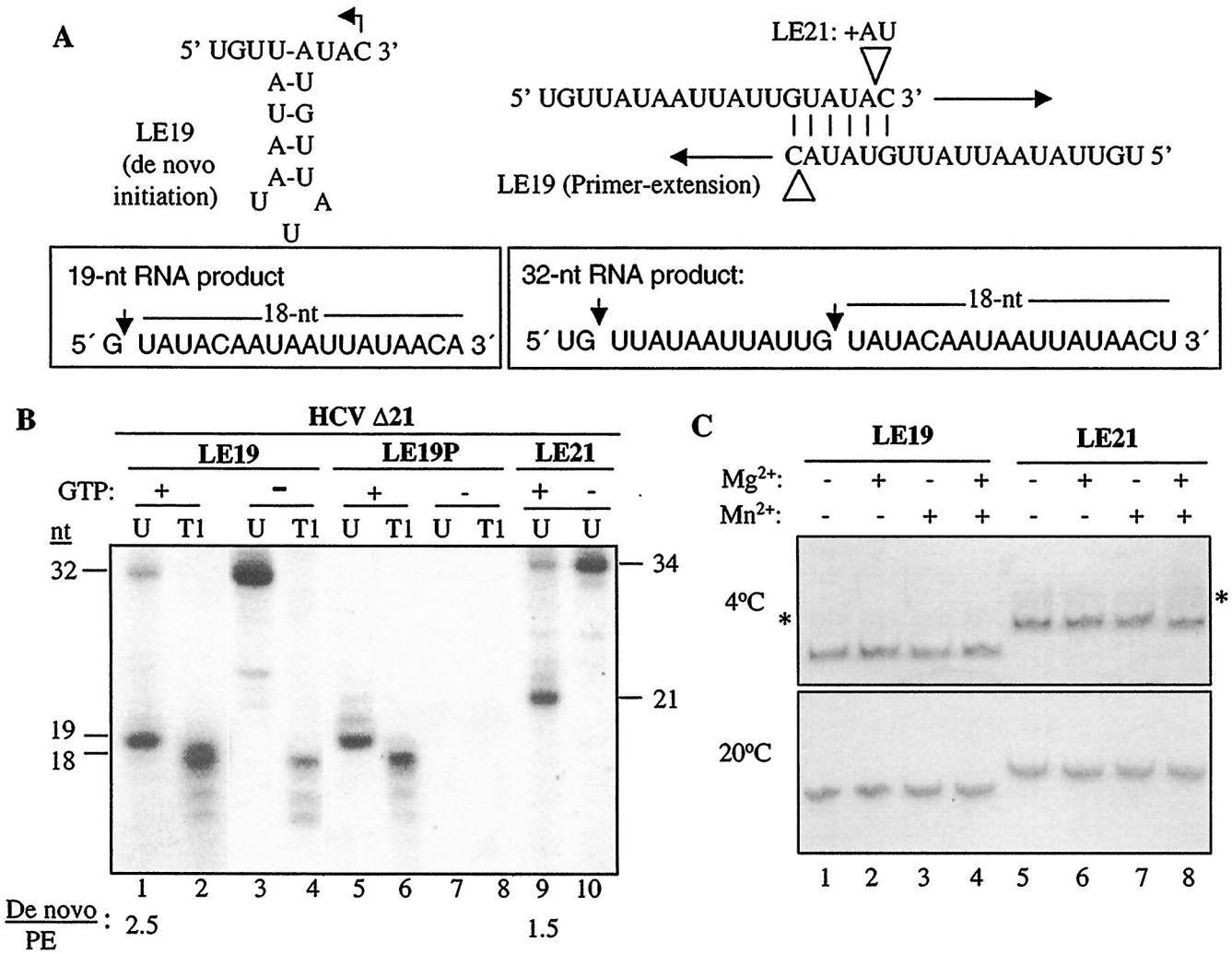

FIG. 2. RNA LE19 and the products that could form by de novo initiation and primer extension. (A) LE19 can form a stem-loop structure that mimics the structure found to be conducive for RNA synthesis (structure on the left) (see reference 14). Two molecules of LE19 could also anneal to allow primer extension from the 3′-most nucleotide of each RNA (structure on the right). In RNA LE21, two nucleotides, A and U, are inserted near the 3′ end (denoted with triangles), increasing the number of base pairs in the heterodimer from six to eight, thus favoring primer extension. The 19-nt product from de novo initiation and the 32-nt product made from primer extension are shown in the boxes. The expected RNase T_1 cleavage sites from these two RNAs are shown with arrows, and the radiolabeled products of 18 nt are identified. (B) Autoradiogram of the products by the HCV RdRp Δ21 from LE19 and LE19P, a modified version of LE19 containing a 3′ puromycin, and LE21. The reactions were performed with (+) or without (−) 200 μM GTP. Reactions in lanes identified by "T1" were treated with RNase T_1, while those in lanes denoted with "U" were untreated. The number of nucleotides in the RdRp products is shown on the sides of the autoradiogram. The ratio of de novo initiation to primer extension (PE) RNA products obtained with LE19 and LE21 is given at the bottom of the autoradiogram. The lengths were identified by comparison to multimeric products of recombination from the BVDV RdRp using templates of 13, 14, 15, and 20 nt (15). (C) The structures of LE19 and LE21 in solution, as analyzed by nondenaturing gel electrophoresis. The analyses used 20% polyacrylamide gel that lacked urea. Two gels were run in parallel, one at 20°C and one at 4°C. All RNAs were in a buffer that contained 100 mM KCl and a 2 mM concentration of the divalent metal indicated above the stained gel. A faint band indicative of higher-order interactions (*) is observed in the gel electrophoresed at 4°C.

right) to form a structure capable of primer extension, the 32-nt primer extension product, based on its sequence, can form in the absence of GTP (Fig. 2A).

In a typical reaction containing Mg^{2+} and Mn^{2+}, the HCV RdRp produced a 19-nt RNA expected from de novo initiation and proper termination as well as a 32-nt RNA that is likely due to primer extension (Fig. 2B, lane 1). In the absence of GTP only the 32-nt RNA was observed, consistent with this RNA being the product of primer extension (Fig. 2B, lane 3). To demonstrate that the 19-nt RNA is indeed due to de novo initiation, we tested a version of LE19 that has a 3′-OH blocked by puromycin (LE19P). LE19P should remain capable of de novo initiation but not primer extension. It did indeed produce the 19-nt de novo-initiated RNA, but not the 32-nt RNA (Fig. 2B, lane 5). To confirm further that the 32-nt RNA originated by primer extension, we used RNase T_1 digestion, which cleaves the phosphodiester bond 3′ of a guanylate (sites of cleavage are shown by arrows in Fig. 2A). Both 19-nt de

novo-initiated and 32-nt primer extension products gave rise to the expected radiolabeled products of 18 nt after digestion (Fig. 2B, lanes 2, 4, and 6). This is consistent with the hypothesis that both the de novo initiation and primer extension reactions could take place within LE19 in one reaction (Fig. 2B, lane 1).

To establish further that primer extension occurs through base pairing at the 3′ termini of two LE19 molecules, we synthesized LE21, which contains an additional two nucleotides, AU, 5′ of the initiation cytidylate. These two nucleotides increase the stability of the heteroduplex between two LE21 molecules (Fig. 2A, schematic on the right) and should produce primer extension and de novo-initiated RNAs of 34 and 21 nt, respectively. LE21 did produce the products of expected sizes (Fig. 2B, lane 9). In the absence of GTP, only the primer extension product of 34 nt was produced (Fig. 2B, lane 10). Furthermore, the ratio of the de novo-initiated RNA to primer-extended RNA was 2.5 with the products from LE19 but was 1.5 with the products from LE21 (compare Fig. 2B, lanes 1 and 9).

Next, we examine whether the structure of LE19 and LE21 are affected by divalent metal ions using native gel electrophoresis, which is highly sensitive to both intra- and intermolecular interactions in RNA molecules (Fig. 2C). Both LE19 and LE21 existed in solution as one predominant conformation. This conformation was not apparently affected by the presence or absence of either 2 mM Mg^{2+} or Mn^{2+} (Fig. 2C, lanes 1 to 8). However, a minor alternative structure was apparent in both LE19 and LE21 when electrophoresis was performed at 4°C, possibly due to intermolecular interactions (denoted with asterisks in Fig. 2C). This alternative conformation is labile to higher temperatures, since the same RNAs electrophoresed at 20°C do not possess this conformation. This result indicates that the effect of the Mg^{2+} and Mn^{2+} on de novo initiation and primer extension is not through an effect on the structures of the RNAs.

Effect of metal ions on RNA synthesis. Reports wherein de novo initiation products were observed (e.g., see reference 13) usually included Mn^{2+} in the reactions. The HCV RdRps purified with buffers lacking divalent metals were used to examine the effects of increasing concentrations of exogenously provided divalent metals. In the absence of exogenously provided metal, no RNA synthesis was observed, as expected (Fig. 3A and B). However, when Mg^{2+} was increased to 0.5 mM, both the primer-extended and the de novo-initiated products were observed, with the primer-extended products being 6- to 12-fold more abundant in several independent experiments (Fig. 3A). Higher Mg^{2+} concentrations further increased both the 21- and the 34-nt products, with the optimal concentration being between 1 and 5 mM. For reactions with Mn^{2+}, the addition of a 0.1 mM concentration of Mn^{2+} produced detectable amounts of both the primer-extended and the de novo-initiated RNAs (Fig. 3B). Unlike the products in reactions with Mg^{2+}, the de novo-initiated RNA was present at a relatively higher abundance (Fig. 3C, lanes 1 to 3 and 10 to 12). Further increases in Mn^{2+} up to 2.5 mM resulted in high levels of RNA synthesis until the concentration was beyond 5 mM, when inhibition of RNA synthesis was observed. These results demonstrate that Mg^{2+} and Mn^{2+} can differentially affect de novo initiation and primer extension. For most of the subsequent reactions, Mg^{2+} was used at either 2 or 4 mM final concentration and Mn^{2+} was used at 2 mM.

In comparison to the HCV RdRp, the BVDV and the GBV RdRps had notable differences in RNA synthesis in response to the presence of divalent metals (Fig. 3C). While the HCV RdRp produced a greater abundance of primer-extended 32-nt RNA from LE19 in comparison to the 19-nt de novo-initiated RNA (Fig. 3C, lane 2), the BVDV and GBV RdRps produced high levels of the de novo-initiated 19-mer in the presence of Mg^{2+} (Fig. 3C, lanes 5 and 8). The addition of 2 mM Mn^{2+} increased the amount of the de novo-initiated RNA by the BVDV RdRp (Fig. 3C, lane 6). However, many of these de novo-initiated products contained one to three nontemplated nucleotides, resulting in a ladder of bands (Fig. 3C, lane 6). At 2 mM, Mn^{2+} was inhibitory to both modes of RNA synthesis by the GBV RdRp (Fig. 3C, lane 9). Reactions with 1 mM Mn^{2+} had less of an inhibitory effect (Ranjith-Kumar et al., unpublished results). When LE21 was used as the template, the primer extension product increased relative to the de novo initiation product for all three RdRps, respectively (Fig. 3C, compare lanes 2, 5, and 8 with lanes 11, 14, and 17). Since RNA syntheses by the three viral RdRps were all performed with the same template and NTP concentrations, the divalent metal is affecting the activity of the RdRps, not just interacting with the substrates for RNA synthesis.

Given the role of Mn^{2+} on RNA synthesis, we tested whether other divalent metals can function differentially in primer extension and de novo initiation. Reactions with all three RdRps in the presence of Ca^{2+}, Co^{2+}, Cu^{2+}, Ni^{2+}, and Zn^{2+} were performed (data not shown). Ca^{2+} at 1 mM supported 3% of the de novo initiation by the BVDV RdRp and 8% of the primer extension product by the HCV RdRp relative to reactions with 1 mM Mn^{2+}, while Co^{2+}, Cu^{2+}, Ni^{2+}, and Zn^{2+} were unable to support either de novo initiation or primer extension by RdRps from HCV and BVDV. The GBV RdRp produced 3% of the de novo-initiated product in 1 mM Co^{2+} as the reaction with 1 mM Mn^{2+}. In all of these reactions, Mg^{2+} and Mn^{2+} were far more active in RNA synthesis by viral RdRps than other metals. RNA synthesis by the HCV RdRp is the focus of the remainder of the work since it had the most dramatically different effects in the presence of Mg^{2+} and/or Mn^{2+}.

Additional characterization of the effects of Mg^{2+} and Mn^{2+}. The dengue virus RdRp exhibited a temperature-dependent change in the ratio of products from de novo initiation versus primer extension (1). To analyze the effect of temperature on HCV RdRp, RNA synthesis reactions were incubated from 15 to 40°C in the presence of 2 mM Mg^{2+}, 2 mM Mn^{2+}, or both (Fig. 4A). At all temperatures tested, de novo-initiated products increased significantly when Mn^{2+} was present (Fig. 4A, lanes 1 to 16). With 2 mM Mg^{2+}, RNA accumulation was maximal at temperatures between 35 to 37°C. However, in reactions with Mn^{2+}, or both Mg^{2+} and Mn^{2+}, the de novo-initiated product was most abundant in reactions performed at 32 to 35°C (Fig. 4A, compare lanes 9 to 16 with lanes 17 to 24). Finally, the de novo initiation product was abundant in reactions with both metals, indicating that Mn^{2+} can independently induce de novo initiation even when Mg^{2+} is present (Fig. 4A, lanes 17 to 24).

RNA synthesis by HCV was reported to take place primarily

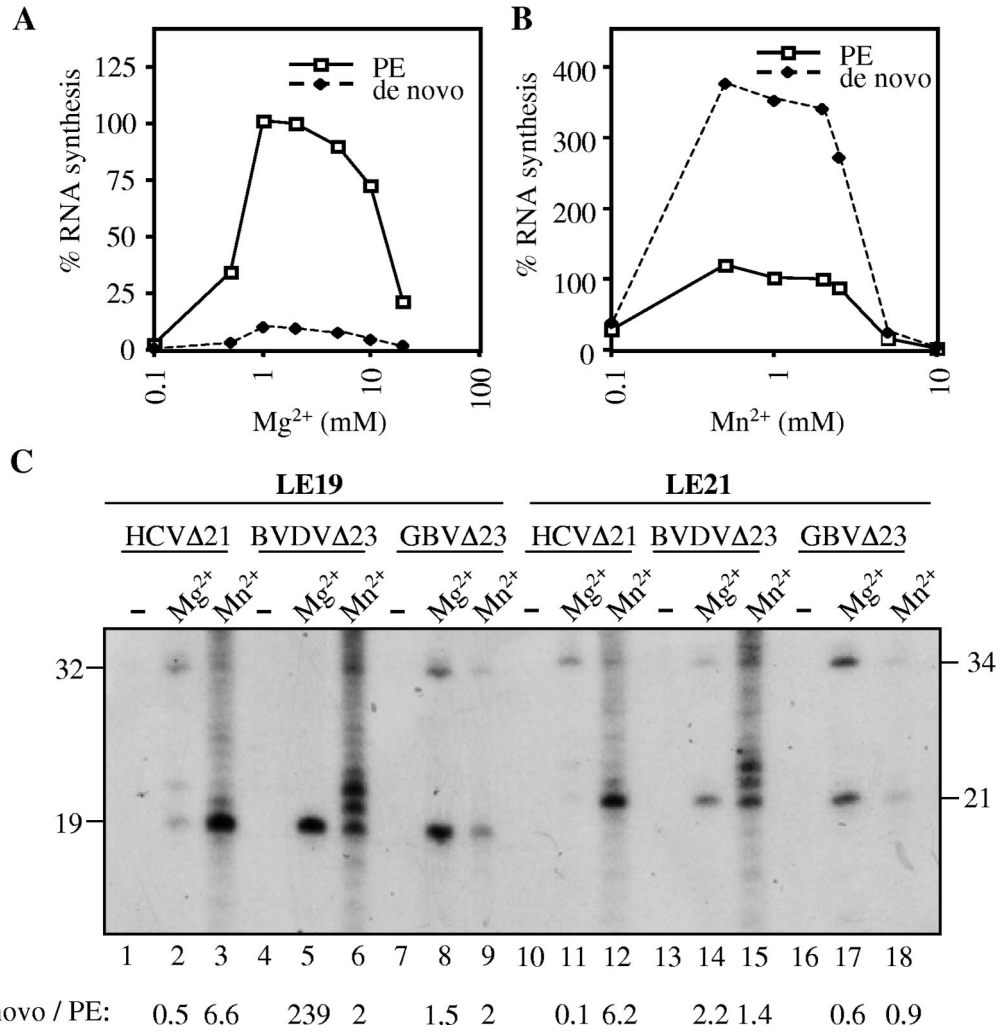

FIG. 3. De novo initiation and primer extension by the three recombinant viral RdRps in the presence of Mg^{2+} or Mn^{2+}. (A) Titration of the effects of increasing Mg^{2+} on RNA synthesis by the HCV RdRp. All RdRp products were normalized to the primer extension (PE) RNA in the reaction mixture with 2 mM Mg^{2+}. (B) Titration of the effects of increasing Mn^{2+} by the HCV RdRp. All RdRp products were normalized to the primer extension (PE) reaction mixture with 2 mM Mn^{2+}. (C) RNA synthesis by the three RdRps (80 nM each). De novo initiation products from LE19 and LE21 are 19 and 21 nt long, respectively, while the primer extension products are 32 or 34 nt long. The ratios of the de novo initiation to the primer extension (PE) products within each reaction are shown below the autoradiogram. −, reaction performed without exogenously provided metal ions.

by oligomeric forms of the RdRp (27, 36). Therefore, RNA synthesis was examined in reactions with increasing amounts of the HCV RdRp (Fig. 4B). In the presence of 2 mM Mg^{2+}, de novo initiation of RNA synthesis was maximal at ~0.48 μM protein (Fig. 4B, lane 7), while primer extension was maximal at ~0.24 μM (Fig. 4B, lane 6). In the presence of Mn^{2+}, de novo initiation increased with higher protein concentrations (Fig. 4B). These results suggest that de novo initiation and primer extension have slightly different requirements.

Effect of metal ions on specificity for de novo initiation. It is possible that Mg^{2+} cannot efficiently effect de novo initiation because primer extension is somehow inhibitory to de novo initiation. To examine this possibility, we performed RNA synthesis with LE19P, which is capable of de novo initiation, but not primer extension (Fig. 2B). In the presence of only Mg^{2+}, synthesis of the 19-nt de novo-initiated RNA was barely above background levels, and the addition of Mn^{2+} increased this product by sevenfold (Fig. 5A). This effect is comparable to that seen with LE19 even though LE19P cannot allow primer extension due to the absence of a 3′ hydroxyl. These results show that Mg^{2+} is incapable of directing de novo initiation efficiently even when primer extension is blocked. Furthermore, Mn^{2+} can induce de novo initiation even in the absence of primer extension.

Earlier studies have shown that a 3′ cytidylate is preferred for de novo initiation of RNA synthesis by the HCV RdRp (14). Whether metal ions influence the specific use of a 3′ cytidylate was examined by comparing rates of synthesis from LE19 and +1U, which contains a 3′ uridylate that is substituted for the cytidylate in LE19 (Fig. 5B). HCV RdRp produced sevenfold more product from LE19 than from +1U in the presence of Mn^{2+}, indicating an inherent, metal-indepen-

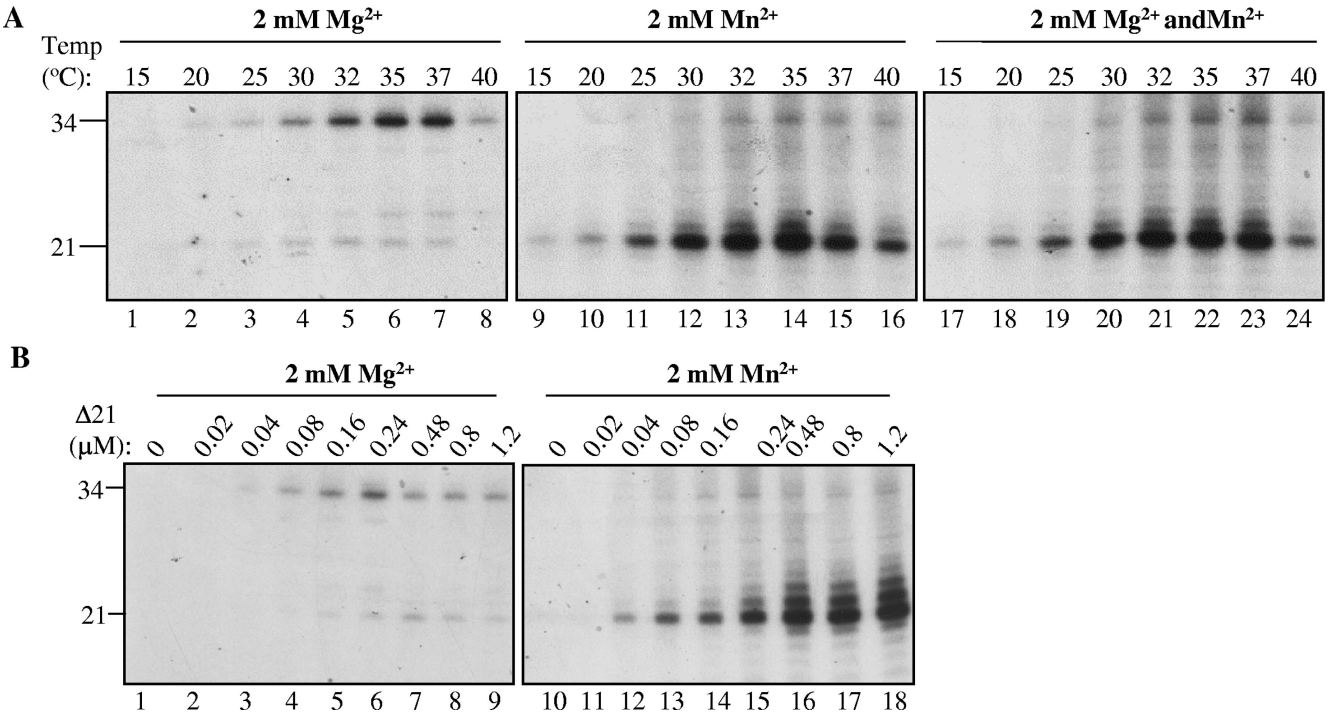

FIG. 4. Characterization of the conditions for efficient de novo initiation and/or primer extension. (A) Effects of increasing temperature on RNA synthesis in the presence of Mg^{2+} or Mn^{2+}. The reaction mixtures contain 80 nM of HCV Δ21 per reaction containing 125 nM template LE21. The sizes of the de novo-initiated (21-nt) and primer-extended (34-nt) RNAs are shown on the left of the autoradiogram. Also shown are effects of different reaction temperatures on RNA synthesis by HCV Δ21 and template LE21. Where added, Mg^{2+} and Mn^{2+} were both at a 2 mM final concentration. In the right-most panel, both divalent metals were used in the reaction. (B) Effect of increasing the amount of HCV Δ21 in the reaction in the presence of 2 mM Mg^{2+} or Mn^{2+}.

dent, preference for a cytidylate as the initiating nucleotide (Fig. 5B, lanes 2, 3, 5, and 6). We attempted to confirm these observations with 14-nt RNAs named 14-C and 14-U, which have a cytidylate and uridylate, respectively, as their 3′-most nucleotide (Fig. 5C). In the presence of Mn^{2+}, 11% of de novo RNA synthesis was observed with 14-U in comparison with 14-C. Reactions with Mg^{2+} produced nearly undetectable amounts of RNA synthesis with 14-U. These results confirm that an initiation cytidylate is preferred for de novo initiation of RNA synthesis irrespective of whether Mg^{2+} or Mn^{2+} ions are present. The specific degrees of recognition of the initiation nucleotide analogs by the HCV, BVDV, and GBV RdRps are compared in more detail in the accompanying manuscript (30).

To investigate further the role of Mn^{2+} ions in de novo initiation, the K_m values for the initiation GTP used in RNA synthesis were determined in the presence of 4 mM Mg^{2+} and 1 mM Mn^{2+} (Fig. 6A), or only 4 mM Mg^{2+} (Fig. 6B). The K_m of GTP for HCV RdRp was 3 ± 0.3 μM in the presence of Mn^{2+} and 103 ± 12 μM in its absence. These results indicate that Mn^{2+} increases the use of GTP for initiation, perhaps by interacting with GTP directly and/or causing a change in the active site of the RdRp. We did not see a significant increase in V_{max} when both metals are present compared to reactions with only Mn^{2+}.

Mn^{2+} increases de novo initiation in reactions with physiological GTP concentrations. The significant differences in K_m values for GTP in the presence and absence of Mn^{2+} suggest that Mn^{2+} could play a more active role in RNA synthesis in vivo when the GTP concentration is limiting. In our reactions, GTP was at 200 μM, twice the K_m for the reaction with only Mg^{2+}. Physiological concentrations of GTP in mammalian cells are estimated to be approximately 0.4 mM (31). To examine the effect of GTP concentration from 0 to 2 mM, RNA synthesis from LE21 was determined in reactions containing Mg^{2+} as the only metal (Fig. 7). As expected, reactions containing no GTP produced mostly the 34-nt primer-extended product (Fig. 7, lane 1). The addition of GTP to 0.1 mM allowed the detection of the de novo-initiated 21-nt RNA (Fig. 7, lane 2). At GTP concentrations up to 2 mM, only a slight increase in amounts of de novo-initiated 21-nt product was observed. The addition of 1 or 2 mM Mn^{2+} to the reaction mixture with 2 mM GTP increased the amount of the de novo-initiated 21-nt RNA by up to 10-fold (Fig. 7, lanes 7 and 8).

Interestingly, increasing the GTP concentration inhibited the production of the primer extension product in a concentration-dependent manner (Fig. 7, lanes 1 to 6). This effect does not require Mn^{2+} and will be more thoroughly examined in a later report.

Mn^{2+} and primer extension. The decrease in primer extension observed in the presence of Mn^{2+} could be due to Mn^{2+} inhibiting primer extension or indirectly decreasing the substrates NTPs available for primer extension by increasing the synthesis of de novo-initiated RNAs. To distinguish between these two possibilities, RNA synthesis reactions were per-

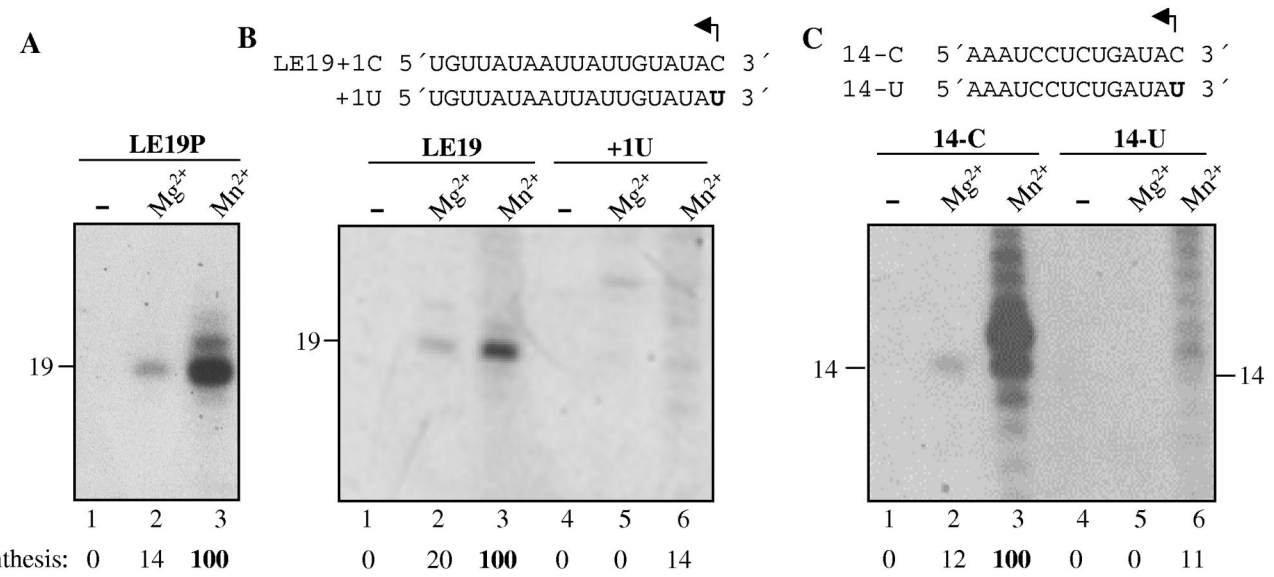

FIG. 5. Effects of divalent metal on specificity for the initiation cytidylate in de novo initiation by HCV Δ21. (A) Mn^{2+} can increase de novo initiation from LE19P, a template incapable of primer extension. (B) Effects of metal on synthesis from LE19 or +1U, a modified LE19 containing an uridylate substituting for the initiation cytidylate. The sequences of the RNAs are shown above the autoradiogram. The initiation cytidylate is denoted with a bent arrow. (C) Effects of metal on synthesis from templates 14-C and 14-U containing, respectively, a 3′ cytidylate or a 3′ uridylate. In all three panels, the results are quantified and normalized to the reaction mixture containing 2 mM Mn^{2+}.

formed in the absence or presence of GTP, which is required for de novo initiation (Fig. 2B). In the absence of GTP, the 34-nt primer extension product was made in reactions containing either Mg^{2+} or Mn^{2+}, indicating that Mn^{2+} could support primer extension (Fig. 8, lanes 4, 5, 8, and 9). When both GTP and Mn^{2+} are present, the primer extension product decreased by 18- to 20-fold relative to that in the reaction that could not initiate de novo (Fig. 8, compare lanes 6 and 7 to lanes 8 and 9). These results indicate that the negative effect Mn^{2+} had on primer extension is likely through a decrease in the available substrates for RNA synthesis.

In these reactions, the de novo-initiated RNA synthesis increased by 14-fold in the presence of Mn^{2+} compared to Mg^{2+} (Fig. 8, compare lanes 2 and 3 to lanes 6 and 7). This increase is likely to be underestimated since we are not quantifying the products of template switch, which also initiated de novo, but were generated by a template switch event due to the ternary polymerase complex not terminating synthesis at the end of the first template (15) (please note the 42-nt RNA in Fig. 8, lanes 6 and 7).

Analyses of mutant HCV RdRps. The observations that Mn^{2+} and Mg^{2+} had different optimal temperatures for de novo initiation and primer extension suggest that they may affect the conformation of the RdRp. This effect would be

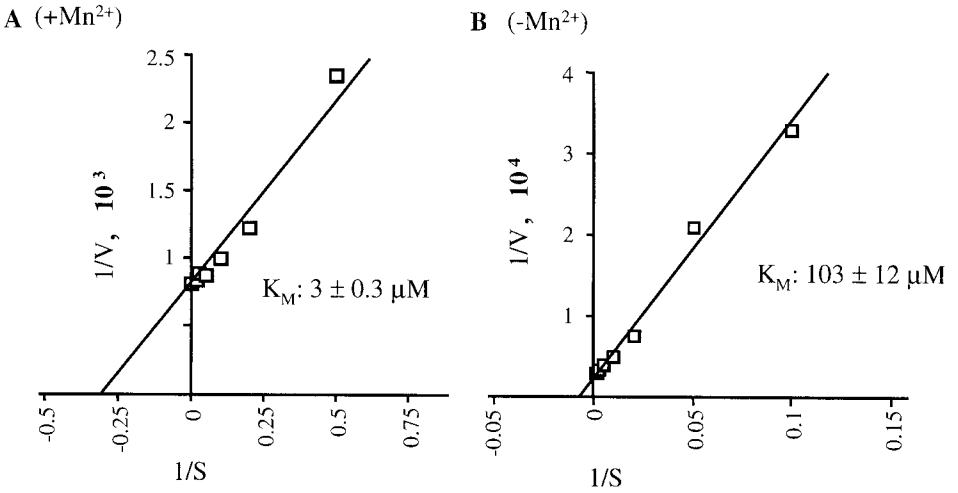

FIG. 6. Mn^{2+} decreases the K_m for GTP. The K_m for GTP as the initiation substrate nucleotide was determined using a Lineweaver-Burke double-reciprocal plot. The K_m is identified from the x intercept. (A) K_m titration performed in the presence of 4 mM Mg^{2+} and 1 mM Mn^{2+}. (B) K_m titration performed in the presence of 4 mM Mg^{2+}.

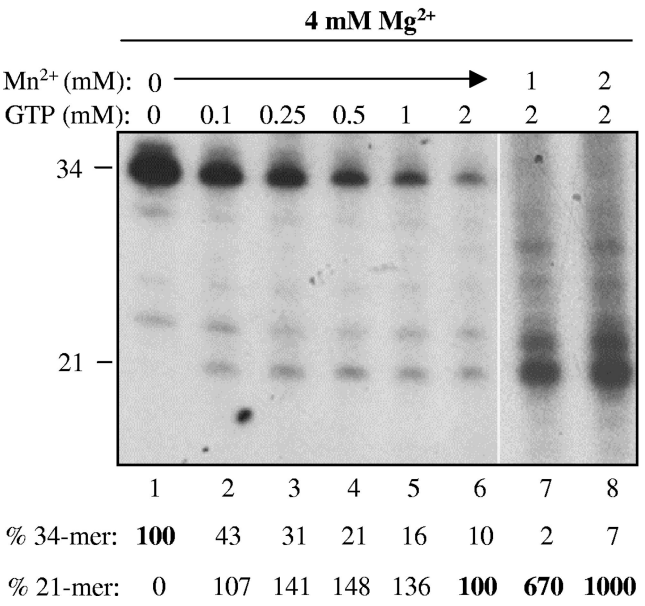

FIG. 7. Effects of GTP concentration on primer extension and de novo initiation. The 34-nt RNA resulted from primer extension, while the 21-nt RNA initiated de novo. Some additional bands between 21 and 34 nt are due to either premature termination of the primer extension or terminal nucleotide addition to LE21. Concentrations of nucleotides are indicated above the autoradiogram. The product in the lane with the number 100 in boldface type was used to normalize products in other lanes. Mn^{2+} can increase de novo initiation in the presence of 2 mM GTP.

consistent with recently published results with the dengue virus replicase and the calicivirus RdRp (1, 22). We seek to obtain more direct evidence for such a change in the HCV RdRp in the presence of Mn^{2+} by mutating regions that could contribute to the formation of the HCV active site, as predicted by the crystal structures of the HCV RdRp (4, 18).

One structure that is likely to be involved in de novo initiation is the β-loop located between amino acids 443 and 454 in the HCV RdRp that protrudes into the catalytic pocket and could play a role in discriminating against double-stranded RNA templates in RNA synthesis (3, 9). Proteins with amino acid substitutions C445A, C445F, Y448A, Y448S, and D444A were produced and tested for RNA synthesis using LE21 in the presence of only Mg^{2+} or both Mg^{2+} and Mn^{2+} (Fig. 9A and B). The ratio of the 21-nt de novo-initiated RNA to the 34-nt primer extension product was determined to assess the relative amount of the two modes of syntheses by each mutant protein (Fig. 9C). Δ21 and all mutant proteins except for Y448S had ratios ranging from 0.06 to 0.19 in the presence of only Mg^{2+} and 3.0 to 6.4 in the presence of both Mg^{2+} and Mn^{2+}. Y448S had a ratio of 0.32 and 30.7 with Mg^{2+} and Mn^{2+}, respectively (Fig. 9C). We note that all of the mutant proteins retained a significant increase in de novo initiation in the presence of Mn^{2+}, indicating that the mutations do not directly affect Mn^{2+} binding (Fig. 9B). It is more likely that the conformation of the structures comprising the active site is affected by this change.

The C-terminal tail of the HCV RdRp is located close to the catalytic site and may play a role in initiation (18). To determine whether it affects the metal requirement in RNA synthesis, we removed 38, 43, and 51 amino acids at the C-terminal portion of the HCV NS5B (Fig. 9A). The truncated proteins, named according to the number of amino acids deleted, were tested for de novo initiation and primer extension in the presence and absence of Mn^{2+} (Fig. 9D). All truncated proteins retained the capability of de novo initiation but were affected in the amount of primer extension products (Fig. 9D), whereas Δ21 and the mutant RdRps produced low but detectable amounts of de novo-initiated product in the presence of only Mg^{2+} (Fig. 9D). Furthermore, while Δ21 had significantly lower primer extension relative to de novo initiation when Mn^{2+} was present, Δ43 and Δ51 retained high levels of primer extension (Fig. 9C).

The activities of Δ51 in the presence of either Mg^{2+} or Mn^{2+} were characterized further (Fig. 10A). Compared to Δ21, Δ51 had higher overall activity for primer extension with increasing Mg^{2+} concentrations (Fig. 10A, lanes 2 to 5, and 3A). Furthermore, primer extension was not inhibited as efficiently as reactions with Δ21 when Mn^{2+} was present in increasing concentrations (Fig. 10A, lanes 6 to 9 and Fig. 3A). To determine the degree to which Mn^{2+} affects primer extension and de novo initiation by Δ51, RNA synthesis reactions were performed in reaction mixtures containing 4 mM Mg^{2+} and various concentrations of Mn^{2+} (Fig. 10B). Primer extension by Δ21 decreased gradually with increasing Mn^{2+} concentration, while de novo initiation increased (Fig. 10B, lanes 1 to 5). In contrast, while primer extension by Δ51 increased upon the

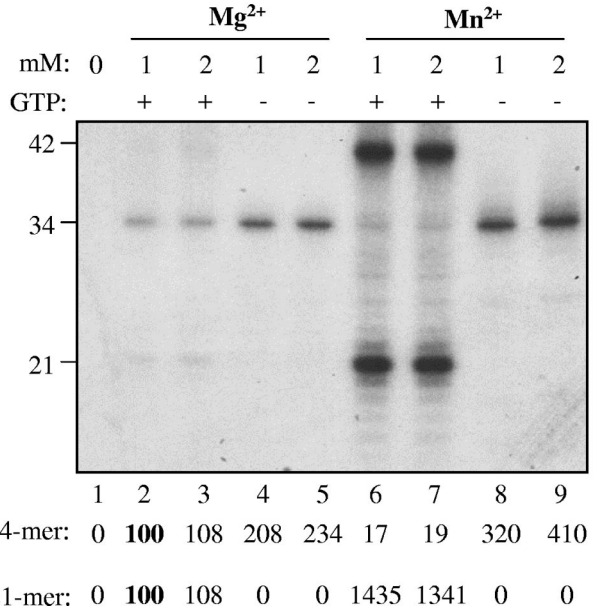

FIG. 8. The effects of Mn^{2+} on primer extension by the HCV Δ21 from template LE21. Conditions used in each reaction are indicated above the autoradiogram. The de novo-initiated RNA is 21 nt, and the primer extension product is 34 nt. The 42-nt RNA is generated by the HCV ternary complex that did not terminate synthesis from LE21 but used a second molecule of LE21 to continue synthesis. This RNA is initiated de novo and is a recombination product. Quantifications of the products synthesized by de novo initiation (the 21-mer) and primer extension (the 34-mer) are shown below the autoradiogram. The product in the lane with the number 100 in boldface type was used to normalize other products.

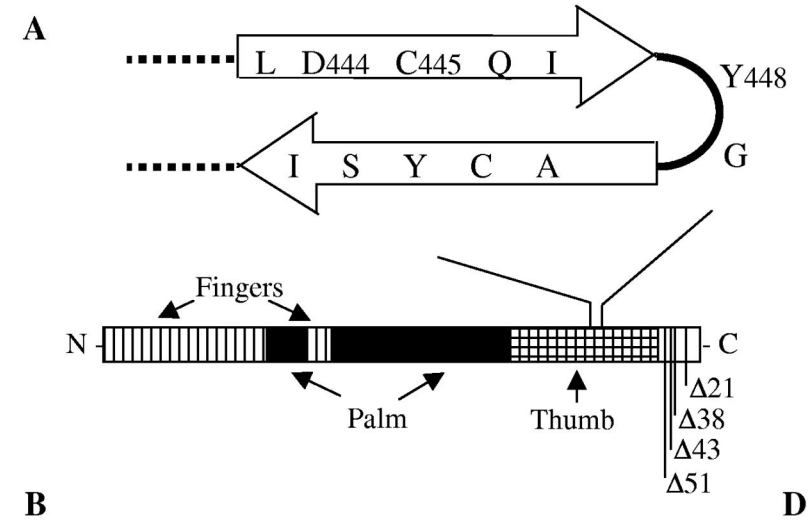

C

Enzyme	*de novo*/PE - Mn^{2+}	*de novo*/PE + Mn^{2+}
Δ21	0.19	6.4
C445A	0.07	3.0
C445F	0.08	4.2
Y448A	0.10	5.6
Y448S	0.32	30.7
D444A	0.06	6.1
Δ38	0.05	4.0
Δ43	0.003	1.7
Δ51	0.002	0.9

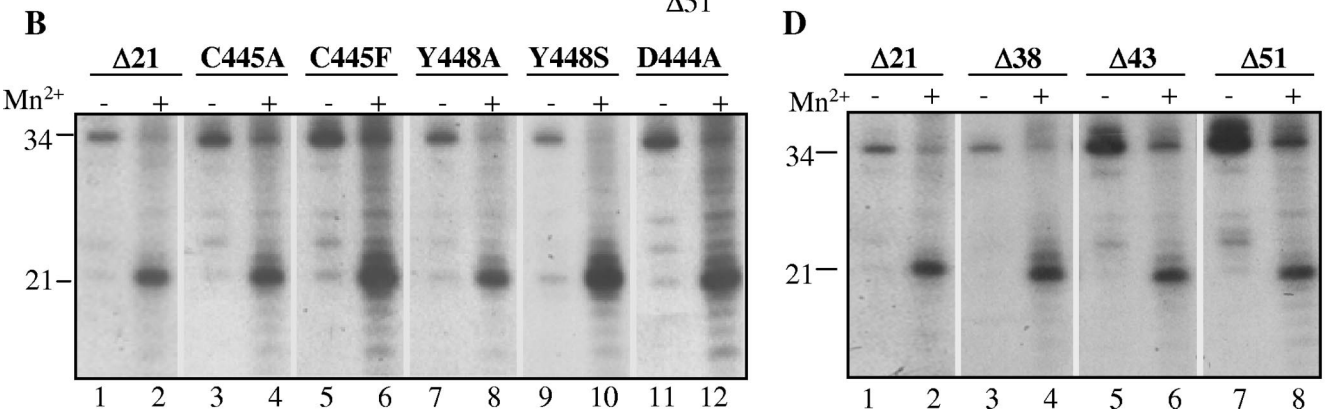

FIG. 9. Effects of mutations within HCV NS5B on de novo initiation and primer extension. (A) At top is shown a schematic of the β-loop within the HCV RdRp that has been reported to affect de novo initiation and primer extension (9). The three amino acids examined by mutational analysis are numbered after the one-letter amino acid code. At bottom is shown a schematic of the relative order of the domains within the primary sequence of HCV RdRp (not to scale). The finger, palm, and thumb subdomains are identified in the figure. Deletions of the region C-terminal to the thumb subdomain are shown as vertical lines to the left of the central bar representing the HCV RdRp. (B) RNA synthesis by HCV Δ21 or select β-loop mutants using template LE21 in the presence of Mg^{2+}, or both Mg^{2+} and Mn^{2+}. All reaction mixtures contained 80 nM RdRp. (C) Ratio of the de novo initiation and primer extension (PE) products made by Δ21 and mutant proteins in the presence of 2 mM Mg^{2+} or 2 mM (each) Mg^{2+} and Mn^{2+}. (D) Autoradiogram demonstrating the effects of C-terminal deletions in the HCV RdRp on the ratio of the de novo-initiated or primer-extended products.

addition of up to 100 μM Mn^{2+}, it decreased with Mn^{2+} concentrations higher than 0.5 mM (Fig. 10B, lanes 6 to 10). Since the Mn^{2+} binding sites in the catalytic pocket are not directly affected by the deletions, the difference between Δ21 and Δ51 suggests that the C terminus responds to binding to Mn^{2+} perhaps by some change in its conformation. It is possible that the C terminus of the HCV RdRp normally participates in concert with the β-loop, in the exclusion of double-stranded templates (40).

Fluorescence spectroscopy analysis. We used the intrinsic fluorescence of the aromatic residues in the HCV RdRp to monitor whether metals induce a detectable change in the HCV Δ21 protein. Fluorescence of aromatic amino acids is highly sensitive to the local environment and is a suitable method of examining conformational changes in proteins (17). Δ21 has nine tryptophans, one of which (Trp^{550}) is located in the C-terminal tail of the HCV NS5B. Δ21 has 21 tyrosine residues, including Tyr^{448} located in the novel β-loop (Fig. 9A) and Tyr^{555} and Tyr^{561} in the C-terminal tail.

The emission spectra of intrinsic tryptophan fluorescence of Δ21 were obtained in the absence and presence of 0.1 and 2.0 mM of Mg^{2+} or Mn^{2+} (Fig. 11A). In these reactions, monovalent salt is included at 300 mM to diminish the effect of nonspecific salt addition to the protein. None of the buffer components, including either Mg^{2+} or Mn^{2+}, produced significant signal under these conditions (Fig. 11A). Furthermore, maximum emission of the tryptophan fluorescence was observed at the expected 340 nm (17). In the presence of 2 mM Mg^{2+} or Mn^{2+}, tryptophan fluorescence decreased by 5 and 7%, respectively, in comparison to that in Δ21 lacking divalent metals (Fig. 11A). Independently acquired spectra of each sample varied by less than 1% in independent measurements. The decrease in tryptophan fluorescence in the presence of Mn^{2+} may reflect some contribution from the quenching of

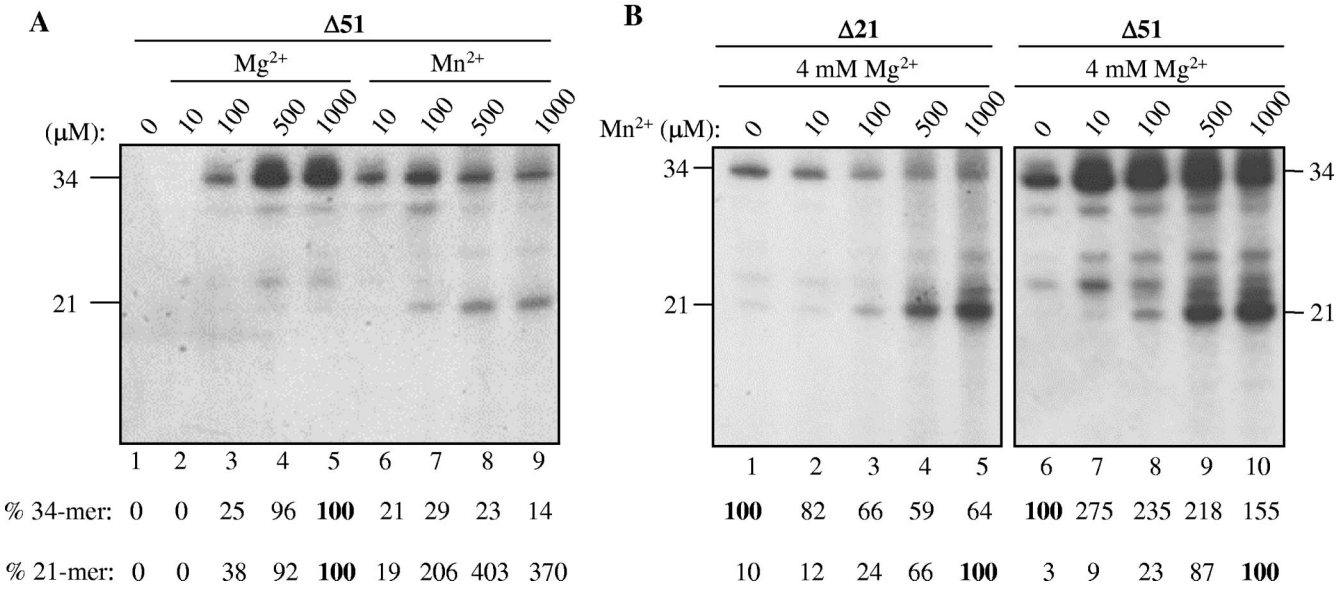

FIG. 10. Comparison of RNA synthesis by Δ51 and Δ21. (A) Effects of increasing concentration of Mg^{2+} or Mn^{2+} using 80 nM Δ51 and 125 nM template LE21. (B) Effects of increasing concentrations of Mn^{2+} on repressing primer extension by an 80 nM concentration of either Δ51 or Δ21 in the presence of 4 mM Mg^{2+}. Lengths of the RdRp products, in nucleotides, are on the sides of the autoradiogram. Quantifications of the products synthesized by de novo initiation (the 21-mer) and primer extension (the 34-mer) are shown below the autoradiogram. The product in the lane with the number 100 in boldface type was used to normalize other products in the autoradiogram.

fluorescence in additional to our proposed conformational change (17).

To confirm the effects of metal on fluorescence spectra of Δ21, we measured intrinsic tyrosine fluorescence. The maximum emission of tyrosine fluorescence was observed at 339 nM, and buffer and metals again did not contribute significantly to the observed spectra (Fig. 11B). In the presence of 2 mM Mg^{2+} or Mn^{2+}, tyrosine fluorescence decreased by 5 and 10%, respectively (Fig. 11B). To our knowledge, Mn^{2+} does not cause nonspecific quenching of tyrosine fluorescence, although the spectra are complicated by some contribution of the tryptophan fluorescence. The results with tryptophan and tyrosine fluorescence are consistent with the hypothesis that both Mg^{2+} and Mn^{2+} can cause a detectable conformational change in the HCV RdRp.

Lastly, to determine whether the effects of Mg^{2+} and Mn^{2+} on the decrease in the fluorescence of the HCV Δ21 are specific, we measured the intrinsic tryptophan fluorescence of the HCV Δ21 in the presence of Ni^{2+} and Co^{2+}, two metals that are incapable of efficiently directing RNA-dependent RNA synthesis. Spectra obtained with 0.1 or 2 mM concentrations of these divalent metals resulted in a $<1\%$ change in the intrinsic fluorescence (Fig. 11C).

DISCUSSION

The HCV RdRp is capable of both primer extension and de novo initiation, with the latter mechanism being more likely to be used to initiate viral RNA synthesis in an infected cell (see reference 13 and references within). We used RNA templates capable of supporting both de novo initiation and primer extension to determine that Mn^{2+} plays an important role in facilitating de novo initiation in vitro. The ability to use Mn^{2+} is especially evident with the HCV RdRp, although similar effects are also seen with the BVDV RdRp. The fact that different RdRps respond differently to metal indicates that this is an inherent property of the flaviviral RdRps.

While divalent metals have well-recognized effects on the template and NTPs, we have observed a small but reproducible effect on the conformation of the HCV RdRp in the absence of template or NTPs. This effect was observed even in the presence of 0.3 M monovalent salt, which should discourage nonspecific ionic interactions. Co^{2+} and Ni^{2+} do not cause a change in the intrinsic fluorescence of the HCV RdRp (Fig. 11). Along with the effects on viral RNA synthesis by mutant HCV RdRp (Fig. 9), Mg^{2+} and Mn^{2+} likely exert their effects at the active site of the polymerase rather than a nonspecific site in the polymerase. The affected region involves at least the β-loop and the C-terminal portion of the RdRp.

Divalent metals are known to modulate substrate selectivity of DNA-dependent RNA polymerases (10, 34). For the HCV RdRp, Mn^{2+} improved the K_m value for the initiation GTP from 103 to 3 μM. Mn^{2+} also decreased primer extension since its addition to reactions containing Mg^{2+} not only increased de novo initiation but also reduced primer extension activity.

An emerging theme in studies of viral RdRp structure and function is that metals can regulate the activities of viral RdRps in addition to performing nucleotide polymerization. The dengue virus replicase was suggested to exist in at least two conformational states that are in dynamic equilibrium (1). The so-called closed conformer, formed at lower temperatures, is more capable of de novo initiation, while the form that preferentially exists at higher temperatures favors primer-dependent synthesis. The crystal structure of the calicivirus RdRp also exists in closed and open conformations that are, respectively, active and inactive for RNA synthesis in vitro (22). The

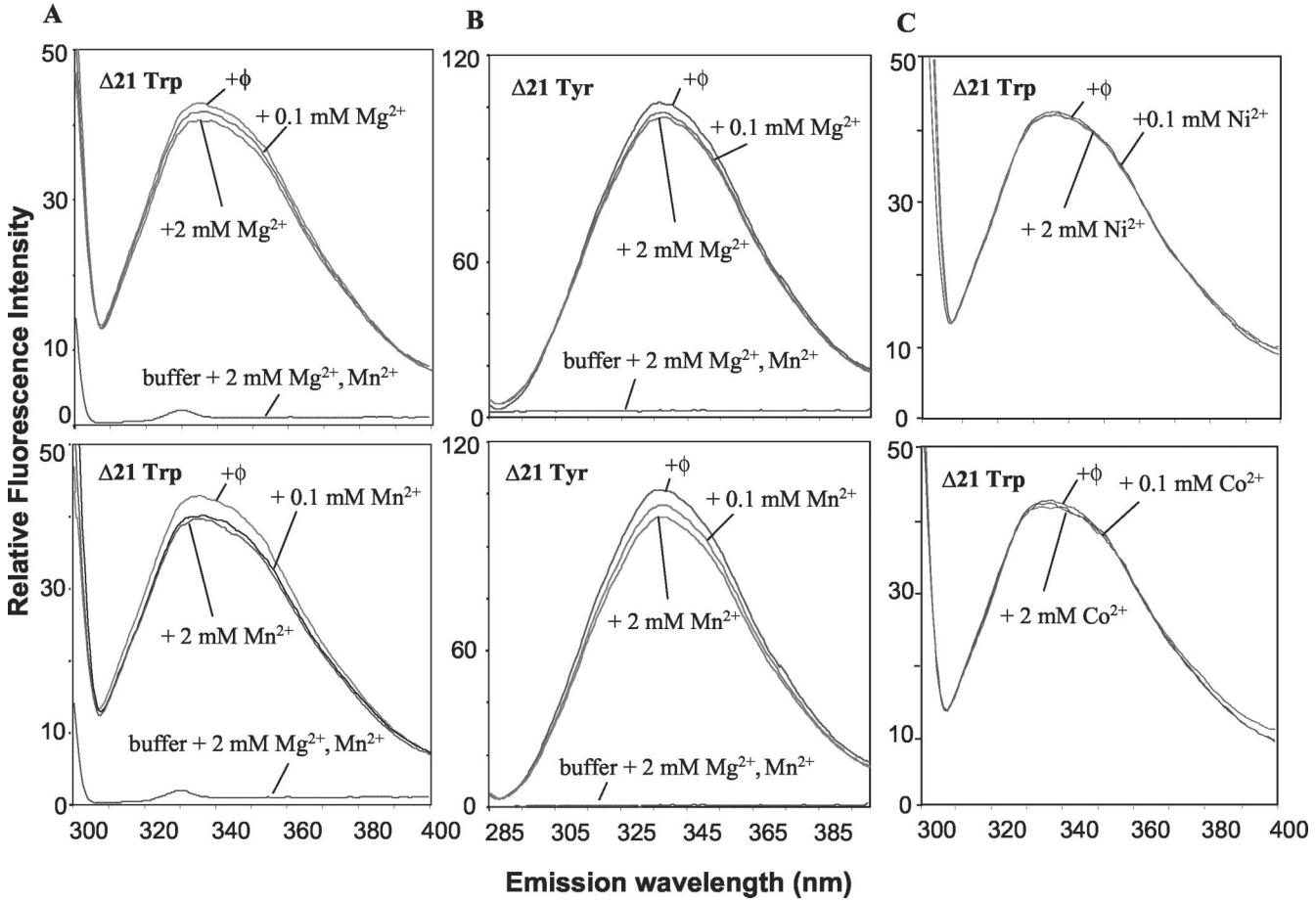

FIG. 11. Intrinsic fluorescence of Δ21 in the absence and presence of divalent metals. (A) Upper panel, tryptophan fluorescence emission spectra of 1 μM HCV Δ21 in the absence of metal and in buffer containing either 0.1 or 2 mM Mg^{2+}. Near the bottom of the graph are the spectra of the buffer used in the measurements amended with 2 mM concentrations of both Mg^{2+} and Mn^{2+}. Lower panel, tryptophan fluorescence of 1 μM HCV Δ21 in the presence of 0, 0.1, or 2 mM Mn^{2+}. (B) Upper panel, tyrosine fluorescence emission spectra of 1 μM Δ21 in the absence of metal, or in buffer containing either 0.1 or 2 mM Mg^{2+}. Near the bottom of the graph are the spectra of the buffers used in the measurements amended with 2 mM of both Mg^{2+} and Mn^{2+}. Lower panel, tyrosine fluorescence of 1 μM Δ21 in the presence of 0, 0.1, or 2 mM Mn^{2+}. (C) Upper panel, tryptophan fluorescence of 1 μM HCV Δ21 in the presence of 0, 0.1, or 2 mM Ni^{2+}. Lower panel, tryptophan fluorescence of 1 μM Δ21 in the presence of 0, 0.1, or 2 mM Co^{2+}.

closed conformer of this RdRp contained two Mn^{2+} ions occupying the active site of the protein. We predict that Mn^{2+} will prove to have a similar effect on the structure of the HCV and possibly other flaviviral RdRps.

The changes induced by metal are likely to be within the HCV RdRp catalytic pocket rather than being a higher-order change such as the oligomerization of the protein (Fig. 12). Dynamic light-scattering experiments to examine the solution radius of the protein revealed that, in the absence of metal, the HCV RdRp exists primarily as a monomer with an average radius of ca. 70 kDa, a good fit with the mass of the HCV RdRp. Addition of metals to the protein did not result in a significant change in the calculate mass of the HCV RdRp (S. Khandekar, unpublished results).

A low-affinity, GTP-specific binding site was recently found between the thumb and finger domains of the HCV RdRp (3) and could affect the oligomerization of the HCV RdRp, a process that may facilitate cooperative RNA synthesis by the HCV RdRp (36). This site is specific for GTP, forming bonds with the base and the ribose. We found that higher concentra-

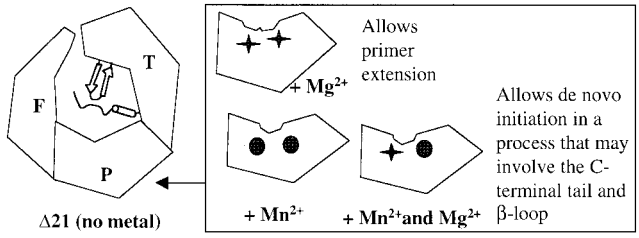

FIG. 12. Model for the modes of RNA synthesis by the HCV RdRp, as modulated by divalent metals. At left is a schematic of the HCV Δ21 protein purified in the absence of metal. While the assumption of the lack of both metals remains to be confirmed by atomic mass absorption experiments, the protein is incapable of either primer extension or de novo initiation of RNA synthesis in the absence of exogenously provided metal ions. The three sections of the cartoon denote the thumb (T), palm (P), and finger (F) domains. The inset shows local conformational changes that take place in HCV Δ21 in the presence of Mg^{2+} and Mn^{2+}. Four-pointed stars denote Mg^{2+} ions, and circles denote Mn^{2+} ions. GTP binding to the junction between T and F domains is hypothesized to narrow the template channel and help exclude a primed template in a reaction that involves the very C-terminal residues of the HCV RdRp.

tions of GTP decreased primer extension (Fig. 7). It remains to be determined whether GTP-binding to the low-affinity site causes a narrowing of the template-binding channel that, along with the β-loop and the C-terminal tail, contribute to the exclusion of primed templates at the active site of the HCV RdRp (Fig. 12). It is likely that several coordinated changes in the RdRp help to discriminate against primed templates, not just the β-loop (9). In support of this claim, Δ21 and all of the HCV proteins we tested that contain an intact β-loop remain perfectly capable of primer extension (Fig. 9) (19, 20).

Could the observed effects of metal have biological relevance? Manganese is known to decrease the specificity for nucleotide incorporation by polymerases (10, 34). Consistent with the effects on DNA-dependent RNA polymerases, we found Mn^{2+} to slightly increase initiation from a 3′ uridylate and expand the use of several GTP analogs for initiation (30). However, Mn^{2+} did not cause the HCV RdRp to lose recognition of the template initiation cytidylate or efficiently use ATP to initiate RNA synthesis (Fig. 5B and C). Also, Mn^{2+} increased RNA synthesis even when GTP concentrations were at least the concentration found inside the cell (Fig. 7). Thus, while Mn^{2+} can be detrimental to high-fidelity RNA replication, it increases the frequency of initiation by at least fivefold. In fact, the quantification of the de novo-initiated product in our assay is likely underestimated since we did not include the products arising from template switch, which also arose from de novo initiation (e.g., as shown in Fig. 8). We observe that higher de novo initiation gives rise to an increased level of template switch in comparison to primer extension, consistent with the observations of Kim and Kao (15).

One proposed reason for Mn^{2+} not being used in viral RNA replication is that it is present at less than 1% of the abundance of Mg^{2+} (28, 39). However, this could be overcome by a higher affinity of the RdRp for Mn^{2+}. Viral and cellular enzymes that specifically use Mn^{2+} as a cofactor have been described previously (26). The higher amount of initiation could overcome any negative selective pressure from a more error-prone RNA synthesis mechanism. In fact, viral RNA replication is an inherently error-prone process (reference 6 and references within). It remains possible that a subset of the RdRps in the cell could contain Mn^{2+} and thus are programmed to be more error prone during synthesis as a way to increase the diversity in the viral population. Alternatively, it is possible that HCV RNA replication is kept at a lower level than is theoretically possible by using only Mg^{2+} as the sole catalytic metal.

ACKNOWLEDGMENTS

We thank the IU Cereal Killers for helpful discussions.

We thank the USDA and the NSF for funding the Kao laboratory. C. C. Kao acknowledges a fellowship from the Linda and Jack Gill Foundation.

REFERENCES

1. **Ackermann, M., and R. Padmanabhan.** 2001. De novo synthesis of RNA by the dengue virus RNA-dependent RNA polymerase exhibits temperature dependence at the initiation, but not the elongation phase. J. Biol. Chem. **276:**39926–39937.
2. **Behrens, S.-E., L. Tomei, and R. De Francesco.** 1996. Identification and properties of the RNA-dependent RNA polymerase of hepatitis C virus. EMBO J. **15:**12–22.
3. **Bressanelli, S., L. Tomei, F. A. Rey, and R. DeFrancesco.** 2002. Structural analysis of the hepatitis C virus RNA polymerase in complex with ribonucleotides. J. Virol. **76:**3482–3492.
4. **Bressanelli, S., L. Tomei, A. Roussel, I. Incitti, R. L. Vitale, M. Mathieu, and R. DeFrancesco.** 1999. Crystal structure of the RNA-dependent RNA polymerase of hepatitis C virus. Proc. Natl. Acad. Sci. USA **96:**13034–13039.
5. **Butcher, S. J., J. M. Grimes, E. V. Makeyev, D. H. Bramford, and D. I. Stuart.** 2001. A mechanism for initiating RNA-dependent RNA polymerization. Nature **410:**235–240.
6. **Elena, S. F., R. Miralles, J. M. Cuevas, P. E. Turner, and A. Moya.** 2000. The two faces of mutation: extinction and adaptation in RNA viruses. IUBMB Life **49:**5–9.
7. **Ferrari, E., J. Wright-Minogue, J. W. S. Fang, B. M. Baroudy, J. Y. N. Lau, and Z. Hong.** 1999. Characterization of soluble hepatitis C virus RNA-dependent RNA polymerase expressed in *Escherichia coli*. J. Virol. **73:**1649–1654.
8. **Honda, A., K. Mizumoto, and A. Ishihama.** 1986. RNA polymerase of influenza virus: dinucleotide-primed initiation of transcription at specific positions on viral RNA. J. Biol. Chem. **261:**5987–5991.
9. **Hong, Z., C. E. Cameron, M. P. Walker, C. Castro, N. Yao, J. Y. Lau, and W. Zhong.** 2001. A novel mechanism to ensure terminal initiation by hepatitis C virus NS5B polymerase. Virology **285:**6–11.
10. **Huang, Y., A. Beaudry, J. McSwiggen, and R. Sousa.** 1997. Determinants of ribose specificity in RNA polymerization: effects of Mn^{2+} and deoxynucleoside monophosphate incorporation into transcripts. Biochemistry **36:**13718–13728.
11. **Joyce, C. M., and T. A. Steitz.** 1995. Polymerase structures and function: variations on a theme? J. Bacteriol. **177:**6321–6329.
12. **Kao, C. C., A. M. Del Vecchio, and W. Zhong.** 1999. De novo initiation of RNA synthesis by a recombinant flaviviridae RNA-dependent RNA polymerase. Virology **253:**1–7.
13. **Kao, C. C., D. Ecker, and P. Singh.** 2001. De novo initiation of viral RNA-dependent RNA synthesis. Virology **287:**252–260.
14. **Kao, C. C., X. Yang, A. Kline, Q. M. Wang, D. Barket, and B. A. Heinz.** 2000. Template requirements for RNA synthesis by a recombinant hepatitis C virus RNA-dependent RNA polymerase. J. Virol. **74:**11121–11128.
15. **Kim, M.-J., and C. C. Kao.** 2001. Factors regulating template switch in vitro by viral RNA-dependent RNA polymerases: implications for RNA-RNA recombination. Proc. Natl. Acad. Sci. USA **98:**4972–4977.
16. **Kim, M.-J., W. Zhong, Z. Hong, and C. C. Kao.** 2000. Template nucleotide moieties for de novo initiation of RNA synthesis by a recombinant RNA-dependent RNA polymerase. J. Virol. **74:**10312–10322.
17. **Lakowicz, J. R.** 1999. Principles of fluorescence spectroscopy, 2nd ed. Kluwer Academic Press, New York, N.Y.
18. **Lesberg, C. A., M. B. Cable, E. Ferrari, Z. Hong, A. F. Mannarino, and P. C. Weber.** 1999. Crystal structure of the RNA-dependent RNA polymerase from hepatitis C virus reveals a fully encircled active site. Nat. Struct. Biol. **6:**937–943.
19. **Lohmann, V., H. Overton, and R. Bartenschlager.** 1999. Selective stimulation of hepatitis C virus and pestivirus NS5B RNA polymerase activity by GTP. J. Biol. Chem. **274:**10807–10815.
20. **Lohmann, V., F. Korner, U. Herian, and R. Bartenschlager.** 1997. Biochemical properties of hepatitis C virus NS5B RNA-dependent RNA polymerase and identification of amino acid sequence motifs essential for enzymatic activity. J. Virol. **71:**8416–8428.
21. **Luo, G., R. K. Hamatake, D. M. Mathis, J. Racela, K. L. Rigat, J. Lemm, and R. J. Colonno.** 2000. De novo initiation of RNA synthesis by the RNA-dependent RNA polymerase (NS5B) of hepatitis C virus. J. Virol. **74:**851–863.
22. **Ng, K., M. Cherney, A. López-Vázquez, A. Machín, J. Alonso, F. Parra, and M. James.** 2002. Crystal structures of active and inactive conformations of a caliciviral RNA-dependent RNA polymerase. J. Biol. Chem. **277:**1381–1387.
23. **Oh, J. W., T. Ito, and M. M. Lai.** 1999. A recombinant hepatitis C virus RNA-dependent RNA polymerase capable of copying the full-length viral RNA. J. Virol. **73:**7694–7702.
24. **Palmenberg, A., and P. Kaesberg.** 1974. Synthesis of complementary strands of heterologous RNAs with Qbeta replicase. Proc. Natl. Acad. Sci. USA **71:**1371–1375.
25. **Paul, A. V., J. H. van Boom, D. Filippov, and E. Wimmer.** 1998. Protein-primed RNA synthesis by purified poliovirus RNA polymerase. Nature **393:**280–284.
26. **Pei, Y., K. Lehman, L. Tian, and S. Shuman.** 2000. Characterization of *Candida albicans* RNA triphosphatase and mutational analysis of its active site. Nucleic Acids Res. **28:**1885–1892.
27. **Qin, W., H. Luo, T. Nomura, N. Hayashi, T. Yamashita, and S. Murakami.** 2002. Oligomeric interaction of hepatitis C virus NS5B is critical for catalytic activity of RNA-dependent RNA polymerase. J. Biol. Chem. **277:**2132–2137.
28. **Quamme, G. A., L.-J. Dai, and S. Rabkin.** 1993. Dynamics of intracellular free Mg^{2+} changes in a vascular smooth muscle cell line. Am. J. Physiol. **265:**H281-H288.
29. **Ranjith-Kumar, C. T., J. Gajewski, L. Gutshall, R. Maley, R. T. Sarisky, and C. Kao.** 2001. Terminal nucleotidyl transferase activity of recombinant fla-

viviridae RNA-dependent RNA polymerases: implication for viral RNA synthesis. J. Virol. **75:**8615–8623.

30. **Ranjith-Kumar, C. T., L. Gutshall, M.-J. Kim, R. T. Sarisky, and C. C. Kao.** 2002. Requirements for de novo initiation of RNA synthesis by recombinant flaviviral RNA-dependent RNA polymerases. J. Virol. **76:**12526–12536.
31. **Schwendel, A., T. Grune, H.-G. Holzhutter, and G. Siems.** 1997. Models for the regulation of purine metabolism in rat hepatocytes: evaluation of tracer kinetic experiments. Am. J. Physiol. **273:**G239-G246.
32. **Sivakumaran, K., C. H. Kim, R. Tayon, and C. Kao.** 1999. RNA sequence and structural determinants for the recognition and efficiency of RNA synthesis by a viral RNA replicase. J. Mol. Biol. **294:**667–682.
33. **Sun, X. L., R. B. Johnson, M. A. Hockman, and Q. M. Wang.** 2000. De novo RNA synthesis catalyzed by HCV RNA-dependent RNA polymerase. Biochem. Biophys. Res. Commun. **268:**798–803.
34. **Tabor, S., and C. Richardson.** 1989. Effect of manganese ions on the incorporation of dideoxynucleotides by bacteriophage T7 DNA polymerase and Escherichia coli DNA polymerase I. Proc. Natl. Acad. Sci. USA **86:**4076–4080.
35. **Van de Sande, J. H., P. C. Loewen, and H. G. Khorana.** 1972. Studies on polynucleotides. 118. A further study of ribonucleotide incorporation into deoxyribonucleic acid chains by deoxyribonucleic acid polymerase I of *Escherichia coli*. J. Biol. Chem. **247:**6140–6148.
36. **Wang, Q. M., M. A. Hockman, K. Staschke, R. B. Johnson, K. A. Case, J. Lu, S. Parson, F. Zhang, R. Rathnachalam, K. Kirkegaard, and J. Colacino.** 2002. Oligomerization and cooperative RNA synthesis activity of hepatitis C virus RNA-dependent RNA polymerase. J. Virol. **76:**3865–3872.
37. **Wang, T. S., and D. Korn.** 1982. Specificity of the catalytic interaction of human DNA polymerase beta with nucleic acid substrates. Biochemistry **21:**1597–1608.
38. **Yamashita, T., S. Kaneko, Y. Shirota, W. Qin, T. Nomura, K. Kobayashi, and S. Murakami.** 1998. RNA-dependent RNA polymerase activity of the soluble recombinant hepatitis C virus NS5B protein truncated at the C-terminal region. J. Biol. Chem. **273:**15479–15486.
39. **Zhang, R., and K. Ellis.** 1989. In vivo measurement of total body magnesium and manganese in rats. Am. J. Physiol. **25:**R1136-R1140.
40. **Zhong, W., E. Ferrari, C. A. Lesburg, D. Maag, A. Gosh, C. Cameron, J. Lau, and Z. Hong.** 2000. Template-primer requirements and single-nucleotide incorporation by hepatitis C virus nonstructural protein 5B polymerase. J. Virol. **74:**9134–9143.